Chemico-Biological Interactions 310 (2019) 108745

Contents lists available at ScienceDirect

Chemico-Biological Interactions

journal homepage: www.elsevier.com/locate/chembioint

UGT-dependent regioselective glucuronidation of ursodeoxycholic acid and obeticholic acid and selective transport of the consequent acyl glucuronides by OATP1B1 and 1B3

Dandan Zhou[a,1], Linghua Kong[a,1], Yiguo Jiang[b], Cheng Wang[b], Yao Ni[a], Yedong Wang[a], Hongjian Zhang[a,**], Jianqing Ruan[a,*]

[a] College of Pharmaceutical Sciences, Soochow University, Suzhou, China
[b] Department of Pharmacy, Suzhou Science & Technology Town Hospital, Suzhou, China

A B S T R A C T

Ursodeoxycholic acid (UDCA) is a major effective constituent of bear bile powder, which is widely used as function food in China and is documented in the Chinese pharmacopoeia as a traditional Chinese medicine. UDCA has been developed as the only accepted therapy by the US FDA for primary biliary cholangitis. Recently, the US FDA granted accelerated approval to obeticholic acid (OCA), a semisynthetic bile acid derivative from chenodeoxycholic acid, for primary biliary cholangitis. However, some perplexing toxicities of UDCA have been reported in the clinic. The present work aimed to investigate the difference between UDCA and OCA in regard to potential metabolic activation through acyl glucuronidation and hepatic accumulation of consequent acyl glucuronides. Our results demonstrated that the metabolic fates of UDCA and OCA were similar. Both UDCA and OCA were predominantly metabolically activated by conjugation to the acyl glucuronide in human liver microsomes. UGT1A3 played a predominant role in the carboxyl glucuronidation of both UDCA and OCA, while UGT2B7 played a major role in their hydroxyl glucuronidation. Further uptake studies revealed that OATP1B1- and 1B3-transfected cells could selectively uptake UDCA acyl glucuronide, but not UDCA, OCA, and OCA acyl glucuronide. In summary, the liver disposition of OCA is different from that of UDCA due to hepatic uptake, and liver accumulation of UDCA acyl glucuronide might be related to the perplexing toxicities of UDCA.

1. Introduction

Bear bile powder is a well-known traditional Chinese medicine documented in the Chinese pharmacopoeia to treat various hepatobiliary disorders. Bear bile is also widely used as function food in China for detoxification and improvement of eyesight for centuries. Ursodeoxycholic acid (UDCA, Fig. 1A) was first identified from the bile of bear in 1902 and was further developed as a modern drug [1]. UDCA is the only accepted therapy by the US FDA for primary biliary cholangitis, a chronic cholestatic liver disease characterized by the destruction of small intrahepatic bile ducts [2,3]. In May 2016, the US FDA granted accelerated approval to obeticholic acid (OCA), a semisynthetic bile acid derivative, for the treatment of primary biliary cholangitis in combination with UDCA in adults with an inadequate response to UDCA, or as monotherapy in adults who cannot tolerate UDCA [4].

In addition to primary biliary cholangitis, UDCA was approved by the US FDA for cholesterol gall stone dissolution and was investigated in a wide range of hepatic and extra-hepatic diseases. However, some perplexing toxicities of UDCA have been reported and include fever, hepatitis, cholangitis, vanishing bile duct syndrome, liver cell failure, severe watery diarrhea, pneumonia, interstitial lung disease, convulsions and mutagenic effects [5]. The toxicities of UDCA remain controversial, and the molecular mechanism of UDCA toxicity has not been well defined yet.

In the liver, UDCA undergoes extensive amino acid conjugation, mainly with glycine and taurine, by amino acid N-acyltransferase (BAAT) to form glycoursodeoxycholic acid and tauroursodeoxycholic acid [6]. In addition to amino acid conjugates, glucuronides of UDCA have been found in the urine of jaundiced patients and exist as not only hydroxyl glucuronide [7] but also acyl glucuronide at the C-24 carboxylic acid [8,9]. Extensive glucuronidation of bile acids might occur when the administered natural bile acids exceed the amidation capacity of the hepatocytes [10,11].

Organic anion transporting polypeptides (OATPs) are a family of important transporters that play a significant role in the *trans*-membrane transport of endogenous molecules, food constituents, drugs and toxins [12]. OATP1B1 and 1B3 belong to the OATP family and are

* Corresponding author. Soochow University, College of Pharmaceutical Sciences, Suzhou, 215123, China.
** Corresponding author. Soochow University, College of Pharmaceutical Sciences, Suzhou, 215123, China.
E-mail addresses: zhanghongjian@suda.edu.cn (H. Zhang), ruanjianqing@suda.edu.cn (J. Ruan).
[1] Zhou Dandan and Kong Linghua equally contribute the work and share the first authorship.

https://doi.org/10.1016/j.cbi.2019.108745
Received 21 November 2018; Received in revised form 25 June 2019; Accepted 8 July 2019
Available online 09 July 2019
0009-2797/

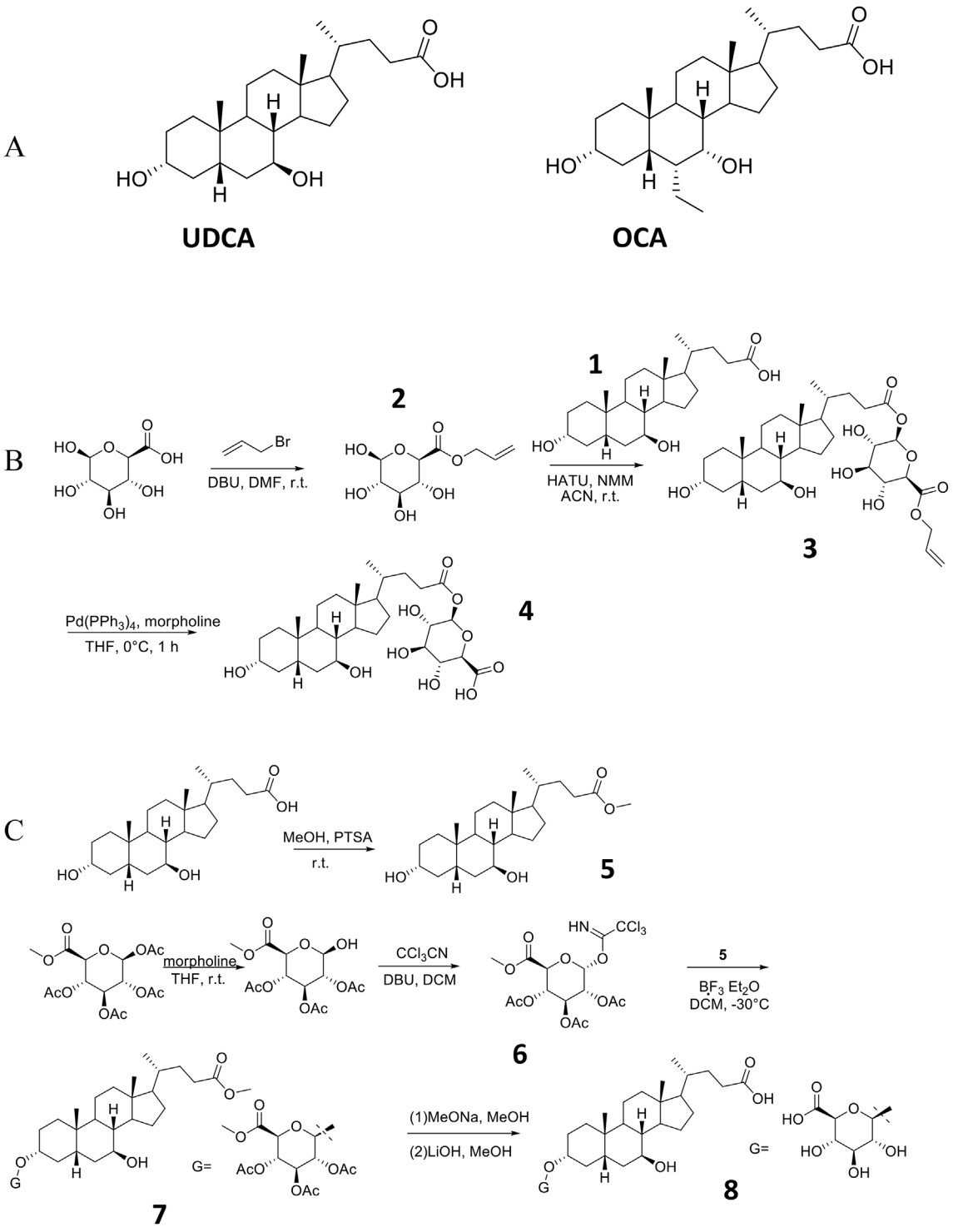

Fig. 1. Chemical structure of UDCA and OCA (A); synthetic method of UDCA acyl glucuronide (B) and UDCA 3-O-hydroxyl glucuronide (C).

exclusively expressed on the basolateral membrane of hepatocytes in normal human liver [13]. It was reported that the uptake of UDCA glycine and taurine conjugates by human hepatocytes was mediated by OATP1B1 and 1B3 [14]. However, the role of OATP1B1 and 1B3 in the transport of UDCA and OCA and their glucuronidation metabolites remains unknown.

Acyl glucuronide conjugates are a series of well-studied reactive metabolites, capable of undergoing molecular acyl migration and covalent binding to proteins/DNAs, which may be associated with the perplexing toxicities of many carboxylic acid-containing drugs. Although the conjugation pathways of UDCA have been studied intermittently since the 1980s, the glucuronidation pathways, especially acyl glucuronidation, have not been well defined. Furthermore, as a new drug, no study has reported on OCA glucuronidation. Therefore, the present study comparatively investigated the glucuronidation of UDCA and OCA in vitro to explore the potential metabolic activation of UDCA and OCA. The regioselectivity of UDCA and OCA glucuronidation by different human uridine 5′-diphospho-glucuronosyltransferases (UGTs) was also examined to identify the major UGT(s) responsible for the glucuronidation of UDCA and OCA. In addition, the potential role of

OATP1B1 and 1B3 in the hepatic uptake of UDCA, OCA, and their glucuronidation metabolites was also studied.

2. Materials and methods

2.1. Materials

UDCA was obtained from Meryer Chemical Technology Co., Ltd. (Shanghai, China). OCA was obtained from Shandong Kangmei Pharmaceutical Technology Co., Ltd. (Shandong, China). Lapatinib was purchased from Chembest Research Laboratories Co., Ltd. (Shanghai, China). Steviol acyl glucuronide was chosen as the internal standard (IS), which was synthesized according to the procedures previously described [15]. Human liver microsomes (HLMs, pooled from 20 different organ donors) and recombinant human UGT isoforms (UGT1A1, UGT1A3, UGT1A4, UGT1A6, UGT1A7, UGT1A8, UGT1A9, UGT1A10, UGT2B4, UGT2B7, UGT2B15 and UGT2B17) were purchased from BD Gentest (Woburn, MA). Alamethicin, L-glutathione reduced, D-saccharic acid 1,4-lactone monohydrate, and formic acid were obtained from Sigma (St. Louis, MO). Uridine diphosphate glucuronic acid (UDPGA) was purchased from Roche (Basel, Switzerland). Dimethylsulfoxide, disodium hydrogen phosphate, and sodium dihydrogen phosphate were purchased from Sinopharm Chemical Reagent co., Ltd. (Shanghai, China). Acetonitrile of HPLC (high performance liquid chromatography) grade was purchased from Merck (Darmstadt, Germany). Ultrawater was purified by Hitech Laboratory water purification systems (Shanghai, China).

2.2. Synthesis of UDCA and OCA glucuronides

The synthetic route of UDCA acyl glucuronide is outlined in Fig. 1B. After reaction with 3-bromoprop-1-ene, allyl glucuronate **2** was synthetized from glucuronide. Condensation of UDCA **1** with allyl glucuronate **2** yielded the allyl glucuronate conjugate **3**. To remove the allyl protection, compound **3** was treated with Pd $(PPh_3)_4$ and morpholine. The deprotected product was precipitated from the solvent, which was filtered and acidified with Amberlyst A-15 (H+) to yield the free UDCA acyl glucuronide **4**. UDCA acyl glucuronide ^{1}H NMR (400 MHz, $CDCl_3$) analysis revealed the following: δ 0.62 (s, 3H, 18-CH_3), 0.93 (d, J = 5.6 Hz, 3H, H-21), 1.13 (s, 3H, 19-CH_3), 2.97 (m, 1H, H-7), 4.45 (m, 1H, H-3), 11.95 (brs, 1H, -COOH).

The synthetic route of OCA acyl glucuronide is the same as that of UDCA acyl glucuronide. After completion of the synthetic process, OCA acyl glucuronide was obtained as a white solid (40 mg). ^{1}H NMR (400 MHz, $CDCl_3 + CD^3OD$) analysis revealed the following: δ 0.61 (s, 3H, 18-CH_3), 0.80–0.83 (m, 6H, 20-CH_3, 19-CH_3), 0.95 (d, J = 6.43 Hz, 3H, 21-CH_3), 3.42 (m, 1H, 3-CH), 3.72 ppm (s, 1H, 7-CH).

The synthetic route of UDCA hydroxyl glucuronide is presented in Fig. 1C. To obtain UDCA methyl ester **5**, a mixture of UDCA and PTSA in MeOH was stirred for 4 h. Methyl 1-O-arylcarbonyl-2,3,4-tri-acetyl-beta-D-glucopyranuronate (compound 6) was produced by reaction of 1,2,3,4-tetra-O-acetyl-beta-D-glucuronate methyl ester with morpholine in anhydrous. Trichloroacetyl glucuronic methyl ester **7** was obtained through stirring compound **6** and 2,2,2-trichloroacetonitrile in DCM, followed by the addition of DBU. Condensation of UDCA methyl ester **5** with trichloroacetyl glucuronic methyl ester **7** yielded the hydroxyl glucuronate conjugate of UDCA methyl ester **8**. To remove the methyl protection, compound **8** was treated with MeONa and LiOH. UDCA 3-O-hydroxyl glucuronide ^{1}H NMR (400 MHz, $CDCl_3$) analysis revealed the following: δ 0.59 (s, 3H, 18-CH_3), 0.93 (d, J = 5.6 Hz, 3H, H-21), 1.13 (s, 3H, 19-CH_3), 3.37 (m, 1H, H-7),4.45 (m, 1H,H-3), 11.95 (brs, 1H, -COOH).

2.3. NMR analysis of UDCA and OCA acyl or hydroxyl glucuronide

The purity and structural integrity of the synthesized UDCA glucuronides were confirmed by LC-MS and proton NMR. Column chromatography was performed using silica gel (100–200 mesh; Qingdao Marine Chemical Inc., Qingdao, China). ^{1}H NMR and ^{13}C NMR spectra were obtained on 400 MHz (Varian) spectrometers. Chemical shifts were given in ppm using tetramethylsilane as the internal standard.

2.4. Glucuronidation of UDCA and OCA in human liver microsomes

The formation of UDCA and OCA glucuronides was examined in HLMs. To obtain the kinetic parameters for UDCA and OCA glucuronidation, different concentrations of UDCA and OCA were incubated with HLMs in 100 mM phosphate buffer (pH 7.4) with 5 mM $MgCl_2$, 25 μg/mL of alamethicin, and 5 mM D-saccharic acid 1, 4-lactone. The reaction was initiated by the addition of 2 mM UDPGA and was incubated at 37 °C for 120 min. The incubation time was set as 120 min according to the linear formation of UDCA and OCA glucuronides. The final volume of the incubation mixture was 100 μL. The reaction was terminated by the addition of 200 μL of cold acetonitrile containing IS.

2.5. Glucuronidation of UDCA and OCA by recombinant human UGT isoforms

To identify human UGT isoform(s) involved in the glucuronidation of UDCA and OCA, 12 recombinant UGT isoforms (UGT1A1, 1A3, 1A4, 1A6, 1A7, 1A8, 1A9, 1A10, 2B4, 2B7, 2B15, and 2B17) were incubated with UDCA and OCA. OCA and UDCA (1 μM) were incubated with 5 mM $MgCl_2$, 0.025 mg/mL of alamethicin, 5 mM saccharolactone and 0.1 mg/mL of UGTs in 100 mM potassium phosphate buffer (pH 7.4). The reaction was initiated by adding 2 mM uridine diphosphoglucuronic acid and incubating for 120 min at 37 °C and then was terminated by adding 200 μl of cold acetonitrile containing 100 nM SVAG (steviol acyl glucuronide). All reactions were conducted in triplicate.

2.6. Kinetics of UDCA and OCA glucuronidation in pooled HLMs and recombinant human UGTs

UDCA ranging from 1 μM to 400 μM was incubated with selected UGT isoforms (UGT1A3, 1A7, 1A8, and 2B7). Meanwhile, OCA ranging from 1 μM to 400 μM was incubated with different UGT isoforms (UGT1A1, 1A3, 1A4, and 2B7). The reaction mixtures consisted of selected UGTs (0.1 mg/mL), 100 mM phosphate buffer (pH 7.4), 5 mM $MgCl_2$, 5 mM D-saccharic acid 1, 4-lactone, and 25 μg/mL of alamethicin. The reactions were initiated by the addition of 2 mM UDPGA, incubated at 37 °C for 2 h, and terminated by adding 200 μl of cold acetonitrile containing 100 nM SVAG. Each experiment was conducted in triplicate.

2.7. Inhibition of UDCA and OCA glucuronidation in UGT1A3 by lapatinib

The inhibition effect of lapatinib from 0.01 μM to 500 μM on UGT1A3-mediated glucuronidation of UDCA and OCA was investigated under the conditions described above. After 120 min of incubation, the reaction was terminated, and samples were prepared and analyzed by LC-MS/MS. Each experiment was conducted in triplicate.

2.8. Uptake of UDCA and UDCA-G1 in hOATP1B1-, 1B3- and NTCP-transfected cells

Cellular uptake of UDCA, OCA, UDCA-G1 and OCA-G1 was investigated using CHO cells stably transfected with hOATP1B1, 1B3 and MDKII cells for NTCP transporters. All CHO cell lines were maintained at 37 °C with 5% CO_2 and 95% humidity in low-glucose Dulbecco's modified Eagle's medium (Hyclone, USA) containing 10% fetal bovine serum (Gibco, USA), 100 U/mL of penicillin and 100 μg/mL of

streptomycin (Hyclone, USA), while MDCKII cell lines were cultured in high-glucose DMEM (Hyclone, USA).

Next, 8×10^4 cells/well were seeded in 24-well culture plates and were grown in medium for four days. The cells were induced with 5 mM sodium butyrate 24 h before the uptake experiments. Uptake experiments were initiated by the addition of 500 μL of UDCA, OCA, UDCA-G1 and OCA-G1 with a defined concentration (10 μM) in HBSS. The cells were then incubated with the test solutions at 37 °C for 2 min. Rosuvastatin (5 μM) was chosen as the prototypical substrate of hOATP1B1 and 1B3, and taurocholate (10 μM) was chosen as the substrate of NTCP. Rifampicin (100 μM) was chosen as the typical inhibitor for hOATP1B1 and 1B3. All the uptake experiments were terminated by aspirating the incubation solution containing test compounds and/or inhibitors and washing the cells with ice-cold HBSS three times. To release compounds taken up in the cells, the cells were repeatedly frozen in a refrigerator at −80 °C and thawed at room temperature three times. Samples were then prepared and analyzed by LC-MS/MS. Additionally, the protein concentration was determined using the BCA Protein Assay Kit (TaKaRa, Japan).

2.9. Sample preparation

All the glucuronidation reactions were terminated by the addition of 200 μL of ice-cold acetonitrile containing 0.1% formic acid and IS. The mixtures were vortexed immediately, followed by centrifugation at 13000 rpm for 10 min. Aliquots of the supernatants were subjected to LC–MS/MS.

2.10. LC–MS/MS analysis

All samples were analyzed by an LC–MS/MS system consisting of an API 4000 Qtrap mass spectrometer equipped with a turbo-V ionization source (Applied Biosystems, Foster City, CA, USA), two LC-20AD pumps with a CBM-20A controller, a DGU-20A solvent degasser, and a SIL-20A autosampler (Shimadzu, Columbia, MD, USA). A Phenomenex Synergi Hydro-RP 80 Å column (75 × 4.6 mm; 4 μm) was used to achieve HPLC separation. The column temperature was held at 40 °C.

For MS/MS quantitation, the API 4000 Qtrap mass spectrometer was operated in the ESI negative mode with multiple reaction-monitoring (MRM). The MS/MS parameters were set as follows: curtain gas, 30 psi; nebulizer gas (GS1), 55 psi; turbo gas (GS2), 55 psi; ion spray voltage, 4500 V; ion source temperature, 450 °C. For the selected ion transitions, the declustering potential (DP) and the collision energy (CE) were optimized. The ion transitions monitored were as follows: OCA, 419.1 → 401.4; OCA acyl glucuronide, 595.5 → 419.4; UDCA, 391.4 → 391.4; UDCA acyl glucuronide, 567.4 → 391.3; UDCA hydroxyl glucuronide, 567.4 → 567.4; the internal standard steviol acyl glucuronide, 493.3 → 317.1. UDCA and OCA acyl glucuronide were quantified by standard calibration curves from 1 to 5000 nM and 1–10000 nM, respectively. The quantitative method displayed good sensitivity and reproducibility. The data were collected and processed using AB Sciex Analyst 1.5.2 data collection and integration software.

2.11. Data analysis

All the data were presented as the means ± SD. Apparent enzyme kinetics by UGTs was obtained by fitting the experimental data with the Michaelis–Menten (eq (1)) model or substrate inhibition (eq (3)) with nonlinear regression analysis using GraphPad Prism 5.0 (GraphPad Software, CA). Assuming a well-stirred model, the in vitro intrinsic hepatic clearance (CL_{int}) was then calculated with eq (2).

The Michaelis–Menten equation:

$$V = (Vmax \times [S])/(Km + [S]) \quad (1)$$

$$CL_{int} = Vmax/Km \quad (2)$$

$$V = Vmax/(1 + Km/[S] + [S]/Ki) \quad (3)$$

where V is the velocity of metabolite formation, Vmax is the maximum velocity, Km is the Michaelis constant defined as the substrate concentration at which the reaction rate is half of Vmax, [S] is the substrate concentration, Ki is the inhibition constant, and CL_{int} is the intrinsic clearance of liver.

The value of Ki was calculated using the Enzyme Kinetics Modules of substrate inhibition Sigma Plot 12.3 based on the Dixon equations [16].

GraphPad Prism 5.0 was used to calculate the IC50 using equation Y = 100/(1 + 10∧((X-LogIC50))).

The data reported represented the average of two or three separate experiments.

3. Results

3.1. Identification of the glucuronidation metabolites of UDCA and OCA in human liver microsomes

When UDCA was incubated with HLMs in the presence of UDPGA, three peaks with the same ion transition of 567.4 → 391.3 were observed in all incubations (Fig. 2A). These three metabolites were tentatively identified as the monoglucuronides of UDCA, corresponding to two monoglucuronides of two hydroxyl groups and one monoglucuronide of acyl group. Comparison with the standard compounds synthesized, the peaks appearing at 3.32 min (UDCA-G1) and at 3.5 min (UDCA-G2) showed the same retention times and MS spectra as UDCA acyl glucuronide and UDCA 3-O-hydroxyl glucuronide standards, respectively. As a result, UDCA-G1 and UDCA-G2 were unambiguously identified as UDCA acyl glucuronide and UDCA 3-O-hydroxyl glucuronide, respectively. UDCA-G3 with a retention time of 3.77 min was tentatively assigned as another UDCA hydroxyl glucuronide. Among these three metabolites, UDCA acyl glucuronide showed a much greater peak area than the other two hydroxyl glucuronides, indicating that HLMs preferentially catalyze glucuronidation of UDCA at the 24-COOH group, rather than at the 3-OH or 6-OH groups.

When OCA was incubated with HLMs in the presence of UDPGA, two additional peaks with the ion transition of 595.5 → 419.4 were observed in all incubations (Fig. 2B), which were absent in controls. Both peaks (named as OCA-G1 and OCA-G2) showed the molecular ion at *m/z* 595, 176 mass units higher than that of OCA (*m/z* 419). Consequently, the two metabolites were tentatively identified as the monoglucuronides of OCA. Compared with the standard compounds synthesized, OCA-G1 showed the same retention time and mass spectra as those of OCA acyl glucuronide. Therefore, the structure of OCA-G1 was unambiguously identified as OCA acyl glucuronide, and the other monoglucuronide of OCA with a retention time of 4.32 min (OCA-G2) was tentatively assigned as OCA hydroxyl glucuronide. The peak area of OCA-G1 was much higher than that of OCA-G2, demonstrating that OCA was predominantly transformed to OCA acyl glucuronide rather than to OCA hydroxyl glucuronide.

3.2. Kinetics of UDCA glucuronidation in human liver microsomes

By incubation with HLMs within the tested substrate concentration range (1–400 μM), OCA and UDCA were mainly metabolized into UDCA-G1 and OCA-G1, respectively. As shown in Fig. 3A, the formation of UDCA-G1 by HLMs followed substrate inhibition kinetics with a Km of 66.75 ± 20.94 μM and Vmax of 18.33 ± 3.34 pmol/min/mg protein, respectively, and a Ki value at 585.1 ± 292.1 μM much higher than the Km, indicating minor inhibition of UDCA on HLMs. The formation of OCA-G1 by HLMs followed typical Michaelis-Menten kinetics with the Km of 79.4 ± 7.14 μM and Vmax of 18.04 ± 0.58 pmol/min/mg protein, respectively. The apparent intrinsic clearance of UDCA in HLMs through acyl glucuronidation was 0.29 ± 0.02 μL/min/mg

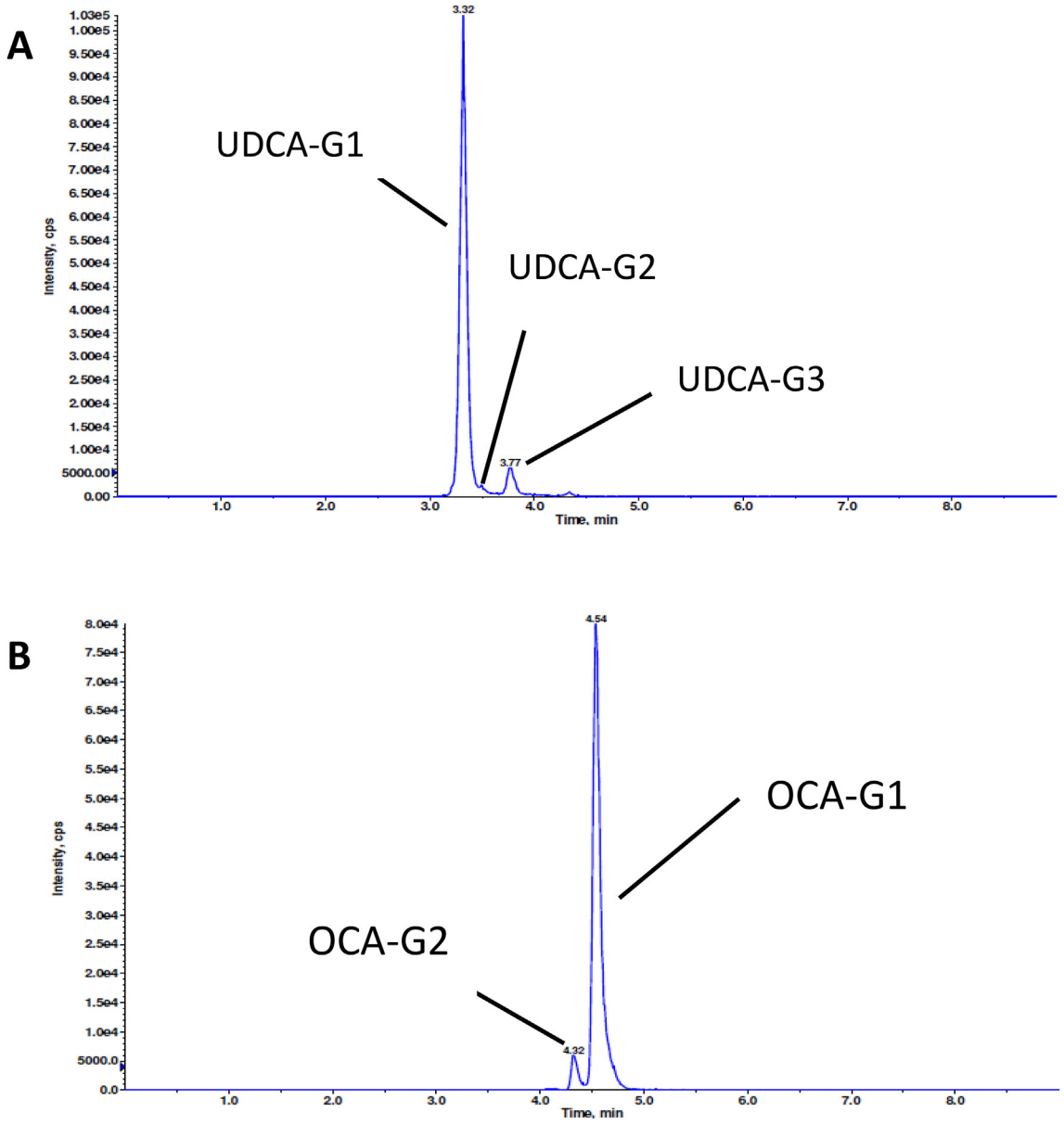

Fig. 2. Representative LC-MS/MS chromatograms of samples obtained from the incubation of 100 μM UDCA (A) and 50 μM OCA (B) with HLMs for 120 min. UDCA-G and OCA-G represent different monoglucuronides of UDCA and OCA, respectively.

protein, and the clearance of OCA in HLMs through acyl glucuronidation was 0.23 ± 0.04 μL/min/mg protein.

3.3. Identification of UGT isoforms involved in the glucuronidation of UDCA and OCA

The relative activities of 12 recombinant human UGT isoforms (UGT 1A1, 1A3, 1A4, 1A6, 1A7, 1A8, 1A9, 1A10, 2B4, 2B7, 2B15, and 2B17) were determined in terms of the formation of UDCA and OCA glucuronides. For UDCA, the acyl glucuronidation was mediated predominantly by UGT 1A3, followed by 1A8, 1A9 and UGT2B7 (Fig. 4A). The hydroxyl glucuronidation of UDCA, including both 3-OH and 6-OH, was mainly mediated by UGT 2B7, as well as 1A3, 1A4 and 2B17 (Fig. 4B and C). OCA acyl glucuronide (OCA-G1) formation was predominantly catalyzed by UGT1A3, followed by UGT1A1 (Fig. 4D). Different from OCA-G1 formation, the OCA-G2 formation was almost solely mediated by UGT1A4 (Fig. 4E).

3.4. Kinetics of UDCA and OCA acyl glucuronidation by human UGTs

The formation of UDCA-G1 mediated by UGT 1A3, 1A8, 1A9 and 2B7 fits substrate inhibition kinetics better than the Michaelis–Menten model, as shown in Fig. 5A–D. UGT 1A3 exhibited the highest Vmax (168.7 ± 16.26 pmol/min/mg protein) and low Km (10.43 ± 2.56 μM) on UDCA-G1 formation. Consequently, UGT 1A3 showed the highest efficiency in catalyzing 24-COOH glucuronidation (CL_{int} 16.18 ± 0.86 μl/min/mg protein, 55 times that of HLMs), followed by UGT 1A8 (4.10 ± 0.77 μL/min/mg protein). UDCA-G1 formation by UGT 1A9 and 2B7 showed similar Vmax and Km values, and, consequently, similar CL_{int} to those of HLMs (Table 1). In addition, UGT 1A8 showed the highest affinity towards UDCA acyl glucuronidation with the lowest Km at 4.10 ± 1.19 μM. However, the Ki value in UGT 1A8 was 27.6 ± 7.6 μM, indicating a high substrate inhibition of UDCA on UGT 1A8.

Within the substrate concentration range tested, only UGT 1A1 and 1A3 catalyzed OCA-1G formation from OCA. As shown in Fig. 5E and F, the acyl glucuronidation of OCA by UGT 1A1 and 1A3 followed typical

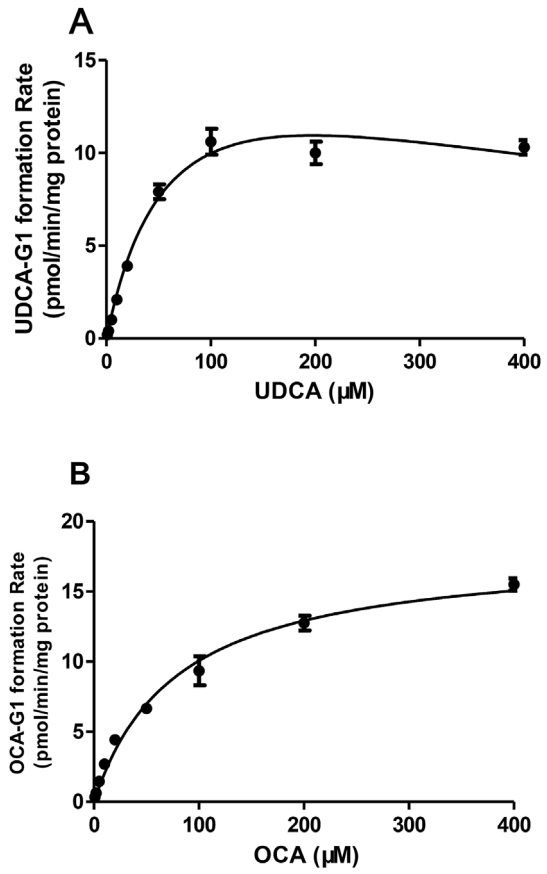

Fig. 3. Effects of the UDCA and OCA concentrations on the formation of UDCA-G1 (A) and OCA-G1 (B) in HLMs. Graph A and B were plotted using substrate inhibition kinetic and typical Michaelis-Menten kinetic equation, respectively.

Michaelis–Menten and substrate inhibition kinetics, respectively. UGT 1A3 displayed a high capacity and affinity (Vmax 138.7 ± 9.42 pmol/min/mg protein, Km 5.08 ± 0.73 μM) in converting OCA to OCA-G1, resulting in a high CL_{int} (27.20 ± 1.34 μL/min/mg protein, 118 times that of HLMs), while UGT1A1 exhibited a much lower capacity (Vmax 32.43 ± 8.95 pmol/min/mg protein) and affinity (Km 84.11 ± 51.9 μM), resulting in a lower CL_{int} (0.38 ± 0.05 μL/min/mg protein).

3.5. Inhibition of UDCA and OCA glucuronidation mediated by UGT1A3

UGT 1A3 plays a significant role in the 24-COOH glucuronidation of both UDCA and OCA. The effect of characteristic inhibitor (lapatinib) of UGT1A3 on UDCA-G1 and OCA-G1 formation was investigated at a series of concentrations from 0.01 μM to 500 μM. As shown in Fig. 6, a potent inhibitory effect of lapatinib toward UDCA and OCA glucuronidation mediated by UGT1A3 was observed, with IC50 values of 1.76 ± 0.10 μM and 2.14 ± 0.30 μM, respectively.

3.6. Uptake of UDCA, UDCA-G1, OCA and OCA-G1 into OATP1B1-, 1B3- and NTCP-transfected cells

As shown in Fig. 7A and B, the uptake values of rosuvastatin (known substrate for OATP1B1 and 1B3) in OATP1B1- and OATP1B3-expressing CHO cells were approximately 6 and 4 times those in vector-transfected control cells, showing good function of OATP1B1 and 1B3 in the transfected cells. The uptake of UDCA by OATP1B1- and 1B3-transfected cells was < 2-folds that by control cells. By contrast, the uptake of UDCA-G1 into OATP1B1 and 1B3 cells was > 7-fold that into control cells, indicating that UDCA-G1 was the substrate for both OATP1B1 and OATP1B3. Coincubation of rifampicin (characteristic inhibitor for both OATP1B1 and 1B3) with UDCA-G1 significantly decreased the uptake of UDCA-G1 by OATP1B1- and 1B3-transfected cells to the level of control cells. However, OATP1B1- and 1B3-expressing cells did not transport OCA or OCA-G1, indicating that both OCA and OCA-G1 were not the substrates of OATP1B1 and 1B3.

Fig. 7C and D shows the uptake of prototypical NTCP substrate taurocholate (TCA) into MDCKII-NTCP cells compared with the respective vector control cells. However, no significant difference was found between the uptake of OCA, UDCA-G1 and OCA-G1 by NTCP-expressing cells and that by the control cells. Uptake of UDCA into MDCKII-NTCP cells was higher than that into the control cells, with an uptake ratio of 1.68-fold (Fig. 7D).

4. Discussion

Bear bile powder is a well-known traditional Chinese health food and medicine and has been widely used in detoxification, pain relief and, particularly, various liver diseases for thousands of years [17]. It has been documented that bear bile possesses anti-allergic, anti-inflammatory, and analgesic properties [18]. Bile acids were regarded as the effective constituents of bear bile, among which UDCA has a high content [19]. In modern medicine, UDCA has been approved by the US FDA as the only pharmacological treatment for primary biliary cholangitis until OCA was licensed in Europe for patients not responsive to UDCA [20].

Previous studies have shown that UDCA could increase bile flow, change the hydrophobicity index of the bile acid pool, and control the levels of serum bilirubin and hepatic transaminases [21–23], indicating that UDCA would be safe and beneficial. However, some “unanticipated” toxicities of UDCA were reported in recent years. In the treatment of primary sclerosing cholangitis with UDCA, more than twice the number of patients died, developed varices, or became eligible for liver transplantation in the UDCA group than in the placebo group [24]. In a study of neonatal and infancy cholestasis, UDCA treatment increased the risk of failure of resolution of cholestasis, life-threatening complications, liver cell failure, and death [25]. Moreover, the incidence of hepatocellular carcinoma increased after UDCA treatment in patients with primary biliary cholangitis, especially in the group of non-responders to UDCA [26]. The safety of UDCA remains controversial, and the molecular mechanism for UDCA toxicity is unclear.

UDCA conjugation with glycine and taurine at the C-24 carboxyl group by BAAT has been extensively studied [27]. However, studies of the UDCA glucuronidation pathway are rather limited. Endogenous bile acids are more easily conjugated with amino acids than with a glucuronosyl group, but exogenously administered UDCA might undergo extensive glucuronidation due to its high dose. In addition, genetic polymorphisms of BAAT had been reported in Japanese [27] and French Caucasian individuals [28] that might cause significant inter-individual variation in the amino acid conjugation of UDCA [29]. Consequently, the glucuronidation pathway might be the major metabolism pathway of UDCA in some individuals with BAAT gene deficiency. In human urine, both UDCA hydroxyl glucuronide and acyl glucuronide were found [8]. However, the UGTs responsible for the different glucuronidation pathways, especially acyl glucuronidation, are still unknown. In the present study, for the first time, our results proved the UGT-dependent regioselective glucuronidation of UDCA towards hydroxyl and carboxyl groups. UGT1A3 showed a predominant role in the carboxyl glucuronidation of UDCA, while UGT2B7 exhibited the highest glucuronidation activity towards both 3-OH and 6-OH of UDCA.

As a new drug, OCA is modified from chenodeoxycholic acid (CDCA) and exhibited much greater potency for farnesoid X receptor activation than CDCA, resulting in reduced bile acid synthesis and improved choleresis [30,31]. The metabolism study of OCA was rather

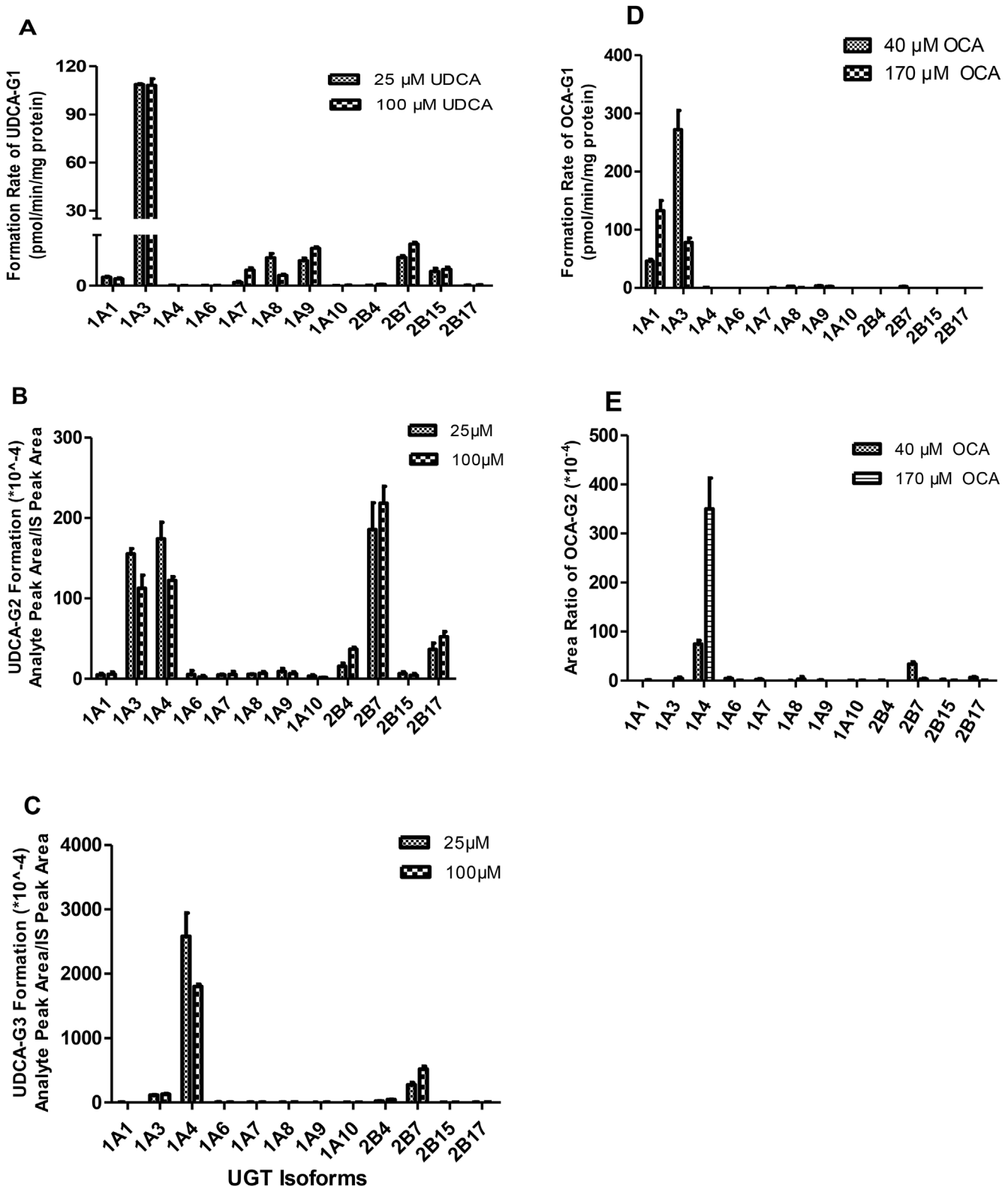

Fig. 4. Formation of UDCA-G1 (A), UDCA-G2 (B), UDCA-G3 (C), OCA-G1 (D) and OCA-G2 (E) by the incubation of UDCA and OCA with recombinant UGTs for 120 min.

limited compared with that of CDCA, and no study was reported on the glucuronidation of OCA. It was demonstrated that CDCA-glucuronide is the most abundant bile acid glucuronide in human serum and urine, which mainly existed as CDCA acyl glucuronide [32,33]. Our study showed that OCA also underwent glucuronidation in HLMs, and the main glucuronide formed was OCA acyl glucuronide. UGT1A3 showed the highest activity and affinity towards OCA acyl glucuronide formation, a finding that was consistent with the result of the study showing CDCA glucuronidation was mainly catalyzed by UGT1A3 [33]. UGT1A1 also played an important role in OCA carboxyl glucuronidation,

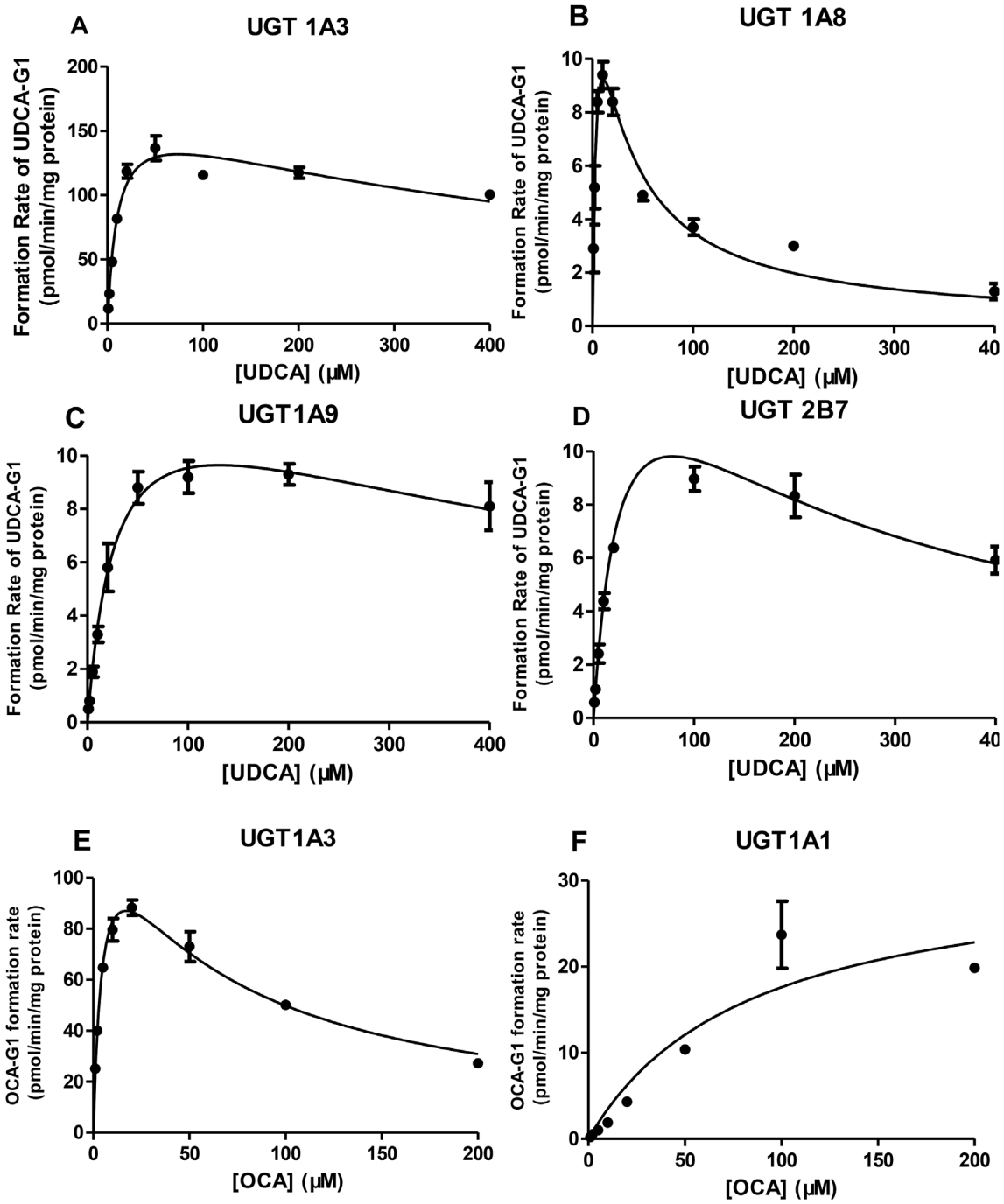

Fig. 5. Effects of the UDCA and OCA concentrations on the formation of UDCA acyl glucuronide by human UGT1A1 (A), UGT1A3 (B), UGT1A9 (C), UGT 2B7 (D), and OCA acyl glucuronidation by human UGT1A3 (E), UGT1A1 (F). All the graphs were plotted using substrate inhibition kinetic equation except graph F using Michaelis-Menten kinetic equation.

Table 1
Kinetics parameters of UDCA and OCA acyl glucuronidation in HLMs and recombinant human UGTs.

		Vmax (pmol/min/mg protein)	Km (μM)	Ki(μM)	CL_{int} (μL/min/mg protein)
UDCA-G1	HLM	18.33 ± 3.34	66.75 ± 20.94	585.1 ± 292.1	0.29 ± 0.02
	UGT1A3	168.7 ± 16.26	10.43 ± 2.56	536.0 ± 191.5	16.18 ± 0.86
	UGT1A8	16.38 ± 2.44	4.10 ± 1.19	27.6 ± 7.6	4.10 ± 0.77
	UGT1A9	13.83 ± 0.86	28.47 ± 3.68	603.9 ± 123.3	0.48 ± 0.05
	UGT2B7	17.03 ± 2.15	28.94 ± 6.58	213.8 ± 56.3	0.58 ± 0.005
OCA-G1	HLM	18.04 ± 0.58	79.4 ± 7.14	–	0.23 ± 0.04
	UGT1A3	138.70 ± 9.42	5.08 ± 0.73	57.8 ± 8.1	27.20 ± 1.34
	UGT1A1	32.43 ± 8.95	84.11 ± 51.9	–	0.38 ± 0.05

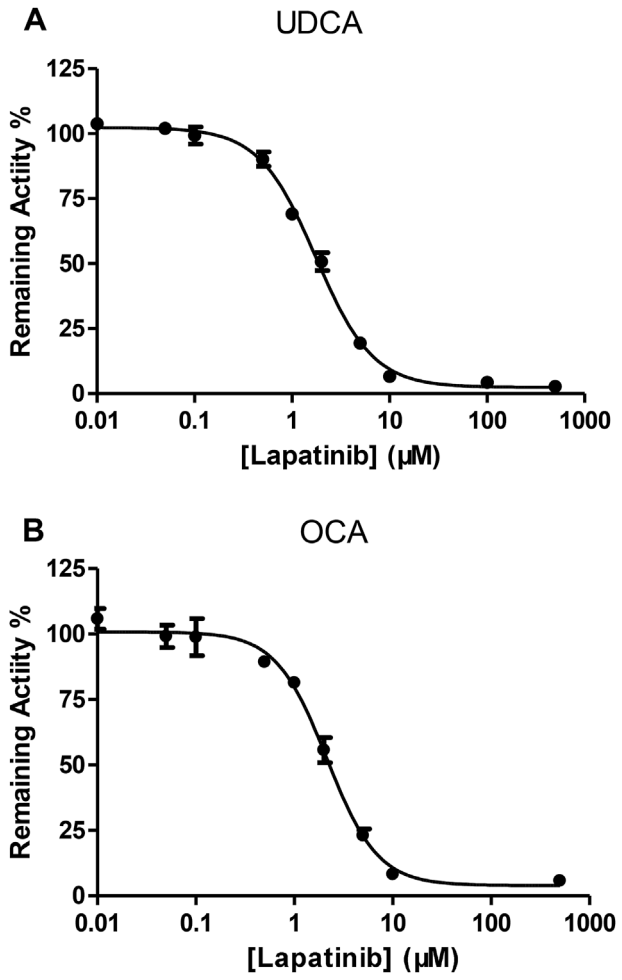

Fig. 6. Inhibition of UDCA (A) and OCA (B) glucuronidation by lapatinib in human UGT1A3. The activity remaining is calculated by regarding the generation rate of UDCA-G1or OCA-G1 without inhibitor as 100%.

especially at high concentrations.

UGT1A3, which is mainly expressed in human liver and intestine, plays an important role in UDCA acyl glucuronidation [34]. UGT1A1, 1A3, 1A4, 1A6 and 1A9 are the major UGTs of the UGT1A family expressed in human liver. The relative expression of hepatic UGT1A3 ranged from 0.2 to 2.4% with significant inter-individual variability [35,36], approximately one-fifth of UGT1A1 and 1A9 expressed in the liver. Our result demonstrated that the apparent clearance of UDCA by UGT1A3 was more than 30 times that by UGT1A9. According to our kinetics results, UGT1A3 is the major enzyme responsible for UDCA acyl glucuronidation, although it is not highly expressed in the liver. Similarly, the apparent clearance of OCA by UGT1A3 was approximately 70 times that by UGT1A1. Thus, UGT1A3 is the major enzyme responsible for both UDCA and OCA acyl glucuronidation.

The extrahepatic UGTs also play important roles in OCA and UDCA glucuronidation. The mRNA expression of UGT1A3 and 2B7 were also detected in the human intestine, but much lower than those in the liver [37]. In addition, Western blot analysis showed that UGT2B7 was faintly detectable in intestinal microsomes [38], indicating that the glucuronidation of OCA and UDCA mainly occurs in the liver. As a result, the present study mainly focused on the investigation of hepatic glucuronidation of OCA and UDCA.

Acyl glucuronide conjugates are reactive metabolites capable of covalent binding to proteins and DNAs [39,40]. Covalent binding to critical proteins, DNAs or some regulatory pathway components by acyl glucuronides might lead to cellular necrosis and result in direct toxicity. On the other hand, acyl glucuronide protein adducts can act as haptens and initiate immune reactions that might lead to immune-mediated toxicity (hypersensitivity reactions) [41]. In our study, we proved that UDCA and OCA were mainly metabolized into acyl glucuronide by UGT1A3. The acyl glucuronide formation of UDCA might be related to the perplexing toxicity of UDCA observed in the clinic, although most studies have focused on the direct toxicity of parent UDCA.

After formation in the hepatocytes, UDCA and OCA glucuronides might be exported to the blood by MRP3 or excreted into bile via efflux transporters. The potential mechanism involved in the efflux of UDCA and OCA has not been revealed in the present study and need further investigation. OATP1B1 and OATP1B3 are specifically expressed in the human liver, where most drug metabolism occurs [42]. Our results demonstrated that OATP1B1 and 1B3 transport UDCA acyl glucuronide, but not the parent UDCA, indicating that hepatocytes selectively uptake UDCA acyl glucuronide rather than UDCA from the blood. It was reported that UDCA could be transported significantly by NTCP, but not by OATP1B1 and OATP1B3, in the transfected cells [43,44], but the uptake ratios were only slightly higher than 100% (less than 1.5-fold), a finding that is consistent with our results that OATP1B1 and 1B3 were not involved in UDCA transport. Consequently, UDCA acyl glucuronide would be accumulated in the liver by uptake through OATP1B1 and 1B3, which could lead to high exposure of UDCA acyl glucuronide in the human liver. Due to the reactivity of acyl glucuronide, the accumulation of UDCA acyl glucuronide in the liver might be related to the liver toxicity observed in the clinic. Our result also proved that, in contrast to UDCA acyl glucuronide, OCA acyl glucuronide was not actively transported by OATP1B1 and 1B3, which would not result in the accumulation of OCA acyl glucuronide in hepatocytes. Consequently, OCA might be a safer drug than UDCA for the treatment of primary biliary cholangitis.

It has been uncovered that nuclear receptor FXR could directly transactivate genes encoding UGTs and indirectly negatively regulate OATP1Bs [45–47]. Our result demonstrated that UGT1A3 and UGT2B7 are mainly responsible for the glucuronidation of UDCA and OCA and OATP1Bs are involved in the absorption of UDCA glucuronide. It is possible that the expression of UGTs and OATP1Bs may be changed over time after dosing of UDCA and OCA repeatedly. Consequently, when OCA and UDCA were prescribed clinically for long time usage, physicians need to take into consideration thedose adjustment.

In conclusion, the present study investigated the roles of human UGTs and OATP1B1 and 1B3 in the disposition of UDCA and OCA. Both UDCA and OCA underwent UGT-dependent regioselective glucuronidation with a positional preference at the carboxyl group. The acyl glucuronidation of UDCA and OCA was predominantly mediated by UGT1A3. The hepatic transporters OATP1B1 and 1B3 selectively transport UDCA acyl glucuronide, but not UDCA, OCA, or OCA acyl glucuronide. The acyl glucuronidation of UDCA and further accumulation of UDCA acyl glucuronide in the liver might be related to the perplexing toxicity caused by UDCA. The liver disposition of OCA acyl glucuronide is different from that of UDCA, which might make OCA a safer drug for the treatment of primary biliary cholangitis.

Conflicts of interest

There are no conflicts to declare.

Declaration of interests

The authors declare that they have no known competing financial interests or personal relationships that could have appeared to influence the work reported in this paper.

Acknowledgements

This work was supported by the National Natural Science

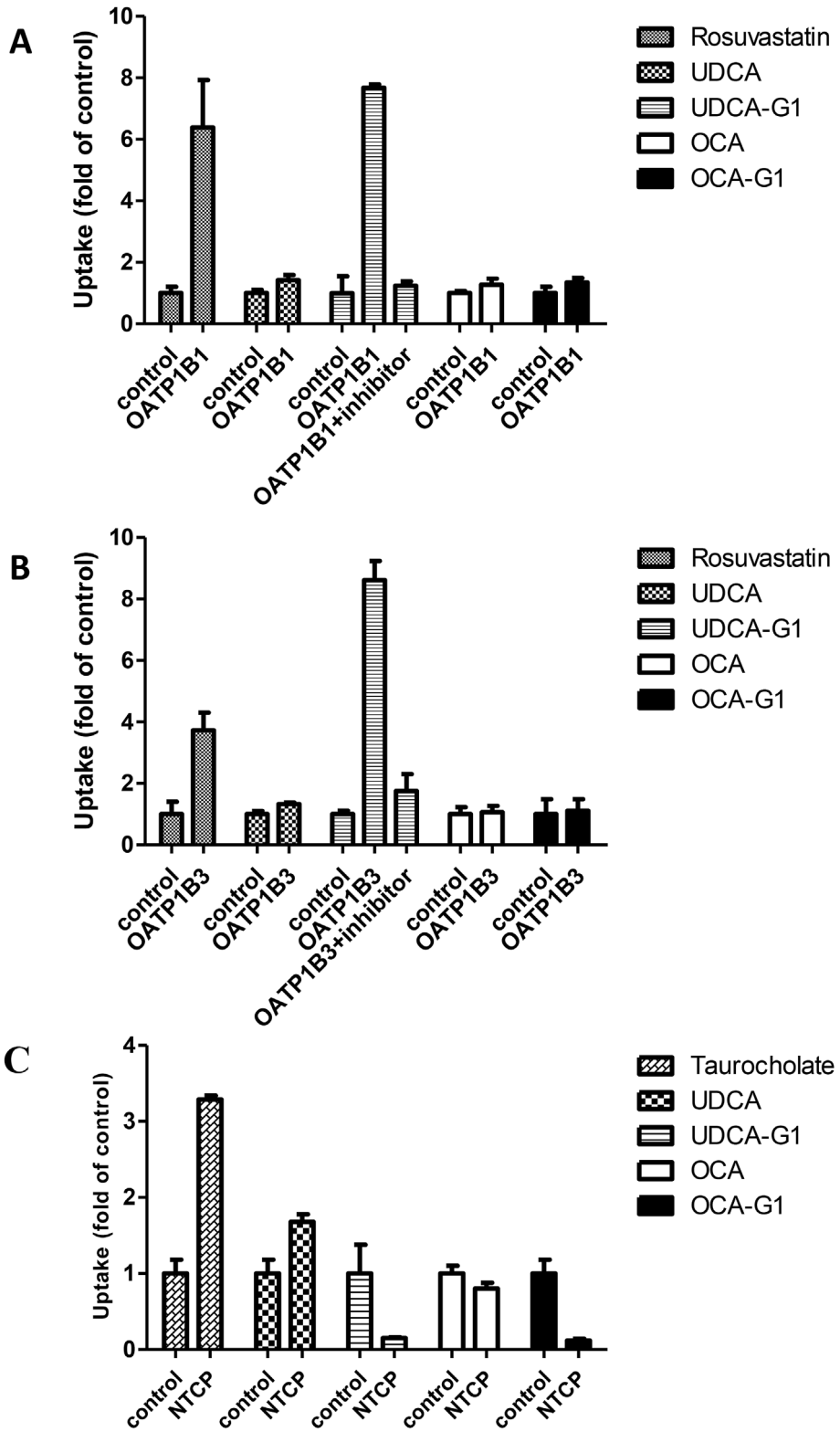

Fig. 7. Uptake of UDCA, UDCA-G1, OCA and OCA-G1 into CHO-OATP1B1 cells (A), CHO-OATP1B3 cells (B), and MDCKII-NTCP cells (C). Control experiments are shown using rosuvastatin as the prototypical OATP1B1 and 1B3 substrate and TCA as the prototypical NTCP substrate. Rifampin (100 μM) was chosen as the prototypical OATP1B1 and 1B3 inhibitor.

Foundation of China (Nos. 81473278 and 81703596) and Jiangsu Province Science Foundation for Youths (BK20150349).

References

[1] I. Makino, H. Tanaka, From a choleretic to an immunomodulator: historical review of ursodeoxycholic acid as a medicament, J. Gastroenterol. Hepatol. 13 (1998) 659–664.
[2] J.A. Talwalkar, K.D. Lindor, Primary biliary cirrhosis, The Lancet 362 (2003)

53–61.
[3] E.J. Carey, A.H. Ali, K.D. Lindor, Primary biliary cirrhosis, Lancet 386 (2015) 1565–1575.
[4] F. Nevens, P. Andreone, G. Mazzella, S.I. Strasser, C. Bowlus, P. Invernizzi, J.P.H. Drenth, P.J. Pockros, J. Regula, U. Beuers, M. Trauner, D.E. Jones, A. Floreani, S. Hohenester, V. Luketic, M. Shiffman, K.J. van Erpecum, V. Vargas, C. Vincent, G.M. Hirschfield, H. Shah, B. Hansen, K.D. Lindor, H.-U. Marschall, K.V. Kowdley, R. Hooshmand-Rad, T. Marmon, S. Sheeron, R. Pencek, L. MacConell, M. Pruzanski, D. Shapiro, A placebo-controlled trial of obeticholic acid in primary biliary cholangitis, N. Engl. J. Med. 375 (2016) 631–643.
[5] M.A. Kotb, Molecular mechanisms of ursodeoxycholic acid toxicity & side effects: ursodeoxycholic acid freezes regeneration & induces hibernation mode, Int. J. Mol. Sci. 13 (2012) 8882–8914.
[6] M. Hu, B.S. Fok, S.-K. Wo, V.H. Lee, Z. Zuo, B. Tomlinson, Effect of common polymorphisms of the farnesoid X receptor and bile acid transporters on the pharmacokinetics of ursodeoxycholic acid, Clin. Exp. Pharmacol. Physiol. 43 (2016) 34–40.
[7] S. Ikegawa, N. Murao, T. Motoyama, T. Yanagihara, T. Niwa, J. Goto, Separation and detection of bile acid 3-glucuronides in human urine by liquid chromatography/electrospray ionization–mass spectrometry, Biomed. Chromatogr. 10 (1996) 313–317.
[8] J. Goto, N. Murao, C. Nakada, T. Motoyama, J. Oohashi, T. Yanagihara, T. Niwa, S. Ikegawa, Separation and characterization of carboxyl-linked glucuronides of bile acids in incubation mixture of rat liver microsomes, Steroids 63 (1998) 186–192.
[9] T. Goto, K.T. Myint, K. Sato, O. Wada, G. Kakiyama, T. Iida, T. Hishinuma, N. Mano, J. Goto, LC/ESI-tandem mass spectrometric determination of bile acid 3-sulfates in human urine: 3β-Sulfooxy-12α-hydroxy-5β-cholanoic acid is an abundant non-amidated sulfate, J. Chromatogr. B: Anal. Technol. Biomed. Life Sci. 846 (2007) 69–77.
[10] A.F. Hofmann, Why bile acid glucuronidation is a minor pathway for conjugation of endogenous bile acids in man, Hepatology 45 (2007) 1083–1084.
[11] H. Takikawa, T. Narita, N. Sano, M. Yamanaka, Glucuronidation of bile acids by their high-dose infusion into rats, Hepatology 13 (1991) 1222–1228.
[12] B. Stieger, B. Hagenbuch, Organic anion-transporting polypeptides, in: M.O. Bevensee (Ed.), Exchangers, 2014, pp. 205–232.
[13] K. Maeda, Organic anion transporting polypeptide (OATP)1B1 and OATP1B3 as important regulators of the pharmacokinetics of substrate drugs, Biol. Pharm. Bull. 38 (2015) 155–168.
[14] K. Maeda, M. Kambara, Y. Tian, A.F. Hofmann, Y. Sugiyama, Uptake of ursodeoxycholate and its conjugates by human hepatocytes: role of Na+-taurocholate cotransporting polypeptide (NTCP), organic anion transporting polypeptide (OATP) 1B1 (OATP-C), and OATP1B3 (OATP8), Mol. Pharm. 3 (2006) 70–77.
[15] M. Wang, J. Lu, J. Li, H. Qi, Y. Wang, H. Zhang, Steviol glucuronidation and its potential interaction with UDP-glucuronosyltransferase 2B7 substrates, Food Chem. Toxicol. 64 (2014) 135–143.
[16] M. Dixon, The graphical determination of K_m and K_i, Biochem. J. 129 (1972) 197–202.
[17] S. Li, H.Y. Tan, N. Wang, M. Hong, L. Li, F. Cheung, Y. Feng, Substitutes for bear bile for the treatment of liver diseases: Research progress and future perspective, J. Evidence-Based Complementary Altern. Med. 2016 (2016) 10.
[18] Y.-w. Li, X.-y. Zhu, P.P.-H. But, H.-W. Yeung, Ethnopharmacology of bear gall bladder: I, J. Ethnopharmacol. 47 (1995) 27–31.
[19] A.C. MacDonald, C.N. Williams, Studies of bile lipids and bile acids of wild North American black bears in Nova Scotia, showing a high content of ursodeoxycholic acid, J. Surg. Res. 38 (1985) 173–179.
[20] C.L. Bowlus, Obeticholic acid for the treatment of primary biliary cholangitis in adult patients: clinical utility and patient selection, Hepatic Med. Evid. Res. 8 (2016) 89–95.
[21] U. Leuschner, M. Leuschner, J. Sieratzki, W. Kurtz, K. Hübner, Gallstone dissolution with ursodeoxycholic acid in patients with chronic active hepatitis and two years follow-up, Dig. Dis. Sci. 30 (1985) 642–649.
[22] C. Degott, E.S. Zafrani, P. Callard, B. Balkau, R.E. Poupon, R. Poupon, Histopathological study of primary biliary cirrhosis and the effect of ursodeoxycholic acid treatment on histology progression, Hepatology 29 (1999) 1007–1012.
[23] K.D. Lindor, Ursodiol for primary sclerosing cholangitis, N. Engl. J. Med. 336 (1997) 691–695.
[24] K.D. Lindor, K.V. Kowdley, V.A.C. Luketic, M.E. Harrison, T. McCashland, A.S. Befeler, D. Harnois, R. Jorgensen, J. Petz, J. Keach, J. Mooney, C. Sargeant, J. Braaten, T. Bernard, D. King, E. Miceli, J. Schmoll, T. Hoskin, P. Thapa, F. Enders, High-dose ursodeoxycholic acid for the treatment of primary sclerosing cholangitis, Hepatology 50 (2009) 808–814.
[25] M.A. Kotb, Ursodeoxycholic acid in neonatal hepatitis and infantile paucity of intrahepatic bile ducts: review of a historical cohort, Dig. Dis. Sci. 54 (2008) 2231–2241.
[26] E.M.M. Kuiper, B.E. Hansen, R.P.R. Adang, C.M.J. van Nieuwkerk, R. Timmer, J.P.H. Drenth, P. Spoelstra, H.T. Brouwer, J.P.H. Kuyvenhoven, H.R. van Buuren, P.B.C.S.G. Dutch, Relatively high risk for hepatocellular carcinoma in patients with primary biliary cirrhosis not responding to ursodeoxycholic acid, Eur. J. Gastroenterol. Hepatol. 22 (2010) 1495–1502.
[27] K. Tougou, T. Fukuda, T. Ito, H. Yamazaki, Y. Fujio, J. Azuma, Genetic polymorphism of bile acid coa: amino acid N-acyltransferase in Japanese individuals, Drug Metab. Pharmacokinet. 22 (2007) 125–128.
[28] C.L. Lino Cardenas, J. Bourgine, C. Cauffiez, D. Allorge, J.M. Lo-Guidice, F. Broly, D. Chevalier, Genetic polymorphisms of glycine N-acyltransferase (GLYAT) in a French caucasian population, Xenobiotica 40 (2010) 853–861.
[29] C.P.S. Badenhorst, R. van der Sluis, E. Erasmus, A.A. van Dijk, Glycine conjugation: importance in metabolism, the role of glycine N-acyltransferase, and factors that influence interindividual variation, Expert Opin. Drug Metabol. Toxicol. 9 (2013) 1139–1153.
[30] U. Beuers, M. Trauner, P. Jansen, R. Poupon, New paradigms in the treatment of hepatic cholestasis: from UDCA to FXR, PXR and beyond, J. Hepatol. 62 (2015) S25–S37.
[31] P. Lefebvre, B. Cariou, F. Lien, F. Kuipers, B. Staels, Role of bile acids and bile acid receptors in metabolic regulation, Physiol. Rev. 89 (2009) 147–191.
[32] J. Trottier, M. Verreault, S. Grepper, D. Monté, J. Bélanger, J. Kaeding, P. Caron, T.T. Inaba, O. Barbier, Human UDP-glucuronosyltransferase (UGT)1A3 enzyme conjugates chenodeoxycholic acid in the liver, Hepatology 44 (2006) 1158–1170.
[33] H. Takikawa, H. Otsuka, T. Beppu, Y. Seyama, T. Yamakawa, Serum concentrations of bile acid glucuronides in hepatobiliary diseases, Digestion 27 (1983) 189–195.
[34] A. Rowland, J.O. Miners, P.I. Mackenzie, The UDP-glucuronosyltransferases: their role in drug metabolism and detoxification, Int. J. Biochem. Cell Biol. 45 (2013) 1121–1132.
[35] M.H. Court, X. Zhang, X. Ding, K.K. Yee, L.M. Hesse, M. Finel, Quantitative distribution of mRNAs encoding the 19 human UDP-glucuronosyltransferase enzymes in 26 adult and 3 fetal tissues, Xenobiotica 42 (2012) 266–277.
[36] T. Izukawa, M. Nakajima, R. Fujiwara, H. Yamanaka, T. Fukami, M. Takamiya, Y. Aoki, S.-i. Ikushiro, T. Sakaki, T. Yokoi, Quantitative analysis of UDP-Glucuronosyltransferase (UGT) 1A and UGT2B expression levels in human livers, Drug Metab. Dispos. 37 (2009) 1759–1768.
[37] C.P. Strassburg, S. Kneip, J. Topp, P. Obermayer-Straub, A. Barut, R.H. Tukey, M.P. Manns, Polymorphic gene regulation and interindividual variation of UDP-glucuronosyltransferase activity in human small intestine, J. Biol. Chem. 275 (2000) 36164–36171.
[38] M.F. Paine, M.B. Fisher, Immunochemical identification of UGT isoforms in human small bowel and in caco-2 cell monolayers, Biochem. Biophys. Res. Commun. 273 (2000) 1053–1057.
[39] A.B. Urs, R.-A. Veronica, NSAID acyl glucuronides and enteropathy, Curr. Drug Metabol. 12 (2011) 245–252.
[40] Y. Yuan, J. Zheng, M. Wang, Y. Li, J. Ruan, H. Zhang, Metabolic activation of rhein: insights into the potential toxicity induced by rhein-containing herbs, J. Agric. Food Chem. 64 (2016) 5742–5750.
[41] H. Horng, H. Spahn-Langguth, L.Z. Benet, Mechanistic role of acyl glucuronides, in: N. Kaplowitz, L.D. DeLeve (Eds.), Drug-Induced Liver Disease, third ed., Academic Press, Boston, 2013, pp. 35–70.
[42] M. Giantin, R.M. Lopparelli, V. Zancanella, P.G. Martin, A. Polizzi, G. Gallina, F. Gottardo, C. Montesissa, L. Ravarotto, T. Pineau, M. Dacasto, Effects of illicit dexamethasone upon hepatic drug metabolizing enzymes and related transcription factors mrnas and their potential use as biomarkers in cattle, J. Agric. Food Chem. 58 (2010) 1342–1349.
[43] J. König, S. Klatt, K. Dilger, M.F. Fromm, Characterization of ursodeoxycholic and norursodeoxycholic acid as substrates of the hepatic uptake transporters OATP1B1, OATP1B3, OATP2B1 and NTCP, Basic Clin. Pharmacol. Toxicol. 111 (2012) 81–86.
[44] K. Maeda, M. Kambara, Y. Tian, A.F. Hofmann, Y. Sugiyama, Uptake of ursodeoxycholate and its conjugates by human hepatocytes: role of Na(+)-taurocholate cotransporting polypeptide (NTCP), organic anion transporting polypeptide (OATP) 1B1 (OATP-C), and oatp1B3 (OATP8), Mol. Pharm. 3 (2006) 70–77.
[45] J.J. Eloranta, G.A. Kullak-Ublick, The role of FXR in disorders of bile acid homeostasis, Physiology 23 (2008) 286–295.
[46] M. Wagner, G. Zollner, M. Trauner, Nuclear receptor regulation of the adaptive response of bile acid transporters in cholestasis, Semin. Liver Dis. 30 (2010) 160–177.
[47] D. Lu, S. Wang, Q. Xie, L. Guo, B. Wu, Transcriptional regulation of human UDP-glucuronosyltransferase 2B10 by farnesoid X receptor in human hepatoma HepG2 cells, Mol. Pharm. 14 (2017) 2899–2907.